A statistical linearization approach to optimal nonlinear energy harvesting

Ian L. Cassidy[a,*] and Jeffrey T. Scruggs[b]

[a]Dept. of Civil & Environmental Engineering, Duke University, Durham, NC, USA
[b]Dept. of Civil & Environmental Engineering, University of Michigan, Ann Arbor, MI, USA

ABSTRACT

In this study, an extension of linear-quadratic-Gaussian (LQG) control theory is used to determine the optimal state feedback controller for a nonlinear energy harvesting system that is driven by a stochastic disturbance. Specifically, the energy harvester is a base-excited single-degree-of-freedom (SDOF) resonant oscillator with an electromagnetic transducer embedded between the ground and moving mass. The electromagnetic transducer used to harvest energy from the SDOF oscillator introduces a nonlinear Coulomb friction force into the system, which must be accounted for in the design of the controller. As such, the development of the optimal controller for this system is based on statistical linearization, whereby the Coulomb friction force is replaced by an equivalent linear viscous damping term, which is calculated from the stationary covariance of the closed-loop system. It is shown that the covariance matrix and optimal feedback gain matrix can be computed by implementing an iterative algorithm involving linear matrix inequalities (LMIs). Simulation results are presented for the SDOF energy harvester in which the performance of the optimal state feedback control law is compared to the performance of the optimal static admittance over a range of disturbance bandwidths.

Keywords: Statistical linearization, optimal control, energy harvesting, vibration

1. INTRODUCTION

Electromechanical systems to harvest energy from ambient mechanical vibrations have become the subject of considerable engineering research. For applications in which the power requirements are on the order of μW–mW, the dominant technology has been comprised of piezoelectric transducers embedded within flexible cantilever beams. For example, it has been shown that such piezoelectric transducers can be used to power wireless sensing and embedded computing systems.[1] However, large-scale energy harvesting from vibrating structures (i.e., vehicles, multi-story buildings, and bridges) has recently been shown to be a viable source of renewable energy. Electromagnetic transducers have been developed to extract power from vibrations in automotive suspensions,[2] railway systems,[3] wave excitations on offshore structures,[4] and wind excitations on buildings.[5] The available power from such applications has been estimated to be at the W–kW scale.

Harvesting energy from vibrations requires circuitry to interface the transducer with storage. The simplest example of a passive energy harvesting circuit is a standard diode bridge. More elaborate active energy harvesting circuits, such as buck-boost converters[6] or H-bridges,[7] are operated via high frequency pulsewidth modulated (PWM) switching control of MOSFETs. The main advantage of active switching converters over passive circuits is that they can impose desired static or dynamic relationships between the voltage and current of the transducer. As such, the input admittance of the circuit can be freely chosen to optimize the rate of power flow from the transducer to storage. Several studies have shown that for sinusoidal disturbances, power generation is optimized by matching the input admittance of the harvesting circuit to the complex conjugate transpose of the driving point admittance (i.e., mobility) of the harvester.[8,9] For the case in which the energy harvester is excited by a stochastic disturbance, Scruggs[9] showed that the optimal causal control of the transducer current (as derived by LQG control theory) is such that the input impedance of the optimal harvesting circuit cannot be made equivalent to any passive network. This is because in such circumstances, there are frequency bands in which the average power for the optimized system flows from storage back into the harvester. That study advocates for the realization of a synthetic dynamic admittance using an actively-controlled H-bridge.

*Further author information: E-mail: ian.cassidy@duke.edu, Telephone: (919) 660-5200

Active and Passive Smart Structures and Integrated Systems 2012,
edited by Henry A. Sodano, Proc. of SPIE Vol. 8341, 834105 · © 2012 SPIE
CCC code: 0277-786X/12/$18 · doi: 10.1117/12.914975

Regardless of the scale or the hardware that is being used to harvest energy, nonlinearities often exist in the vibrating structure and transducer. In a recent study by Stanton *et al*,[10] a nonlinear model for a piezoelectric energy harvester is derived from first principles and is compared to an experimental system. It is shown that nonlinear damping in the cantilever beam as well as nonlinear electromechanical coupling in the piezoelectric patch must be accounted for in the model in order to accurately predict the response of the beam. In addition, Cassidy *el al*[11] developed a predictive model to account for the nonlinearities present in an electromagnetic transducer consisting of a ballscrew actuator coupled to a permanent-magnetic synchronous machine. The nonlinearities in that device are caused by the sliding friction interaction between the ballscrew and ball bearings as well as the elasticity of the belt that connects the ballscrew to the shaft of the motor.

The main objective of this paper is to develop a way to account for dynamic nonlinearities in the harvester, while optimizing the controller for maximum power generation. Toward this end we use statistical linearization to account for the influence of the nonlinearities on the stochastic response. This concept has been applied in piezoelectric energy harvesting applications by Ali *et al*,[12] but not in the context of optimal control. However, problems involving simultaneous statistical linearization and optimal control have been investigated in other applications. These techniques were first developed to account for saturation constraints on control inputs in stochastic systems.[13] In another study by Gökçek *et al*,[14] saturating linear-quadratic-regulator (SLQR) and saturating linear-quadratic-Gaussian (SLQG) feedback gains were developed for linear systems with saturating actuators. Several additional studies[15,16] have developed sub-optimal control designs to account for nonlinear systems that are subjected to stochastic disturbances.

In this paper, the control objective is different from the ones presented in.[13–16] The performance objective in those studies minimizes the variance of the system's output, while the performance objective in the present study maximizes the average power generated by the transducer. Furthermore, the nonlinearity in the energy harvesting system in this study is a result of Coulomb friction present in the electromagnetic transducer, which was experimentally identified by Cassidy *el al*.[11] We show that the optimal feedback gains for the nonlinear system can be computed by solving two nonlinear, coupled algebraic equations. The first equation is similar to the standard Lyapunov equation, which is used to solve for the stationary covariance matrix, while the second equation is similar to the standard Riccati equation, which is used to solve for the optimal feedback gains. Solving these two equations can be accomplished through an iterative algorithm, which solves the Riccati equation using standard linear matrix inequality (LMI) techniques.[17]

2. ENERGY HARVESTER MODEL

An illustration of the electromagnetic transducer that is considered in this study is shown in figure 1(a). Linear-to-rotational conversion is accomplished via a precision ballscrew. Such devices constitute one of the most efficient methods of linear-to-rotational conversion when power flow is in the direction from linear to rotational motion and when high mechanical advantage is important. The ballscrew is interfaced with the shaft of a permanent-magnet synchronous machine via a timing belt with a 1:1 ratio. The configuration shown, in which the motor is placed in tandem with the screw could be replaced by a configuration in which the motor shaft is mounted directly to the rotating screw. Typically, these types of transducers are used for positioning in the manufacturing industry and are commercially available, for example, from Kollmorgen.[18]

The linear velocity $\dot{x}(t)$ of the device is related to the angular velocity of the motor $\dot{\theta}(t)$ via the lead conversion l; i.e., $\dot{x}(t) = l\dot{\theta}(t)$. The linear-to-rotational conversion of the ballscrew can be modeled as relating the linear force $f(t)$ of the device to the electromechanical force $f_e(t)$ of the motor, via the equation

$$f(t) = f_e(t) - F_c \mathrm{sgn}\left(\dot{x}(t)\right) - m_d\ddot{x}(t) - c_d\dot{x}(t) - k_d x(t) \tag{1}$$

where m_d and c_d are the equivalent linear mass and viscous damping resulting from the rotational inertia and viscous damping of the ballscrew and shaft of the motor, respectively. It was experimentally observed in Cassidy *et al*[11] that Coulomb friction and stiffness forces, which are represented by F_c and k_d, are also present in the device. For the transducer considered in this study, it can be shown that the electromechanical force is proportional to current via the relationship

$$f_e(t) = \frac{3K_e}{2l} i(t) = c_e i(t) \tag{2}$$

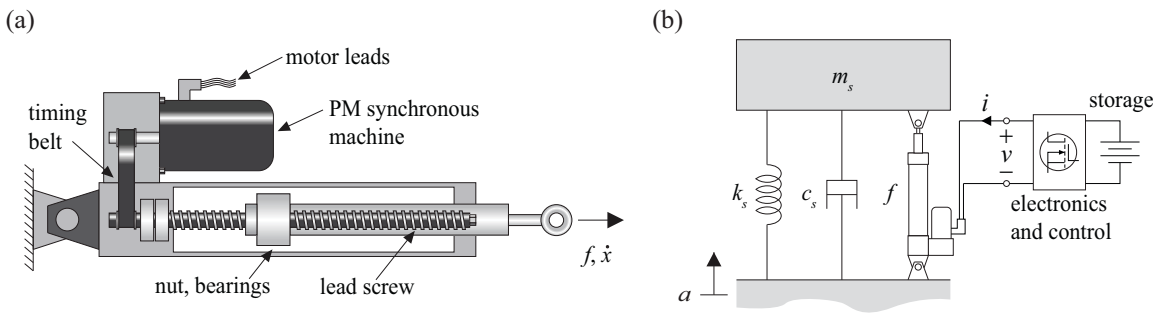

Figure 1. (a) Illustration of the electromagnetic transducer, consisting of a back-driven ballscrew and a permanent magnet synchronous machine; (b) SDOF oscillator and coupled electromagnetic transducer, which is connected to electronics and energy storage.

where K_e is the magnitude of the back-emf of the motor and c_e is the electromechanical coupling coefficient. From the relationship in equation (2), the voltage generated by the transducer is proportional to linear velocity; i.e., $v(t) = c_e\dot{x}(t)$.

Next, we consider an energy harvesting system consisting of the electromagnetic transducer embedded within a single-degree-of-freedom (SDOF) resonant oscillator as shown in figure 1(b). The SDOF oscillator is characterized by a mass m_s, a damping c_s, and a stiffness k_s, and is excited at its base by the stochastic disturbance acceleration $a(t)$. Thus, the coupled dynamics of the SDOF oscillator and electromagnetic transducer can be expressed by the nonlinear differential equation

$$m\ddot{x}(t) + c\dot{x}(t) + kx(t) + F_c\text{sgn}\left(\dot{x}(t)\right) = m_s a(t) + f_e(t) \tag{3}$$

where $x(t)$ is the relative displacement of the mass of the structure, $m = m_d + m_s$, $c = c_d + c_s$, and $k = k_d + k_s$. If we define the harvester state vector as

$$\mathbf{x}_h(t) = \begin{bmatrix} \sqrt{k} & 0 \\ 0 & \sqrt{m} \end{bmatrix} \begin{bmatrix} x(t) \\ \dot{x}(t) \end{bmatrix} \tag{4}$$

then the harvester dynamics can be expressed by the self-dual state space

$$\dot{\mathbf{x}}_h(t) = \mathbf{A}_h\mathbf{x}_h(t) + \mathbf{F}_h\text{sgn}\left(\dot{x}(t)\right) + \mathbf{B}_h i(t) + \mathbf{G}_h a(t) \tag{5a}$$

$$v(t) = \mathbf{B}_h^T\mathbf{x}_h(t) \tag{5b}$$

$$\dot{x}(t) = \mathbf{C}_h\mathbf{x}_h(t) \tag{5c}$$

where

$$\mathbf{A}_h = \begin{bmatrix} 0 & \sqrt{k/m} \\ -\sqrt{k/m} & -c/m \end{bmatrix}, \qquad \mathbf{B}_h = \begin{bmatrix} 0 \\ c_e/\sqrt{m} \end{bmatrix}, \qquad \mathbf{G}_h = \begin{bmatrix} 0 \\ m_s/\sqrt{m} \end{bmatrix},$$

$$\mathbf{F}_h = \begin{bmatrix} 0 \\ -F_c/\sqrt{m} \end{bmatrix}, \qquad \mathbf{C}_h = \begin{bmatrix} 0 & 1/\sqrt{m} \end{bmatrix}.$$

In many vibratory energy harvesting applications, the disturbance acceleration is most accurately modeled as a broadband stochastic process. As such, we characterize the disturbance acceleration by the second-order bandpass filter

$$\dot{\mathbf{x}}_a(t) = \mathbf{A}_a\mathbf{x}_a(t) + \mathbf{B}_a w(t) \tag{6a}$$

$$a(t) = \mathbf{C}_a\mathbf{x}_a(t) \tag{6b}$$

where

$$\mathbf{A}_a = \begin{bmatrix} 0 & 1 \\ -\omega_a^2 & -2\zeta_a\omega_a \end{bmatrix}, \qquad \mathbf{B}_a = \begin{bmatrix} 0 \\ 2\sigma_a\sqrt{\zeta_a\omega_a} \end{bmatrix}, \qquad \mathbf{C}_a = \begin{bmatrix} 0 & 1 \end{bmatrix}.$$

Table 1. Parameter values for the electromagnetic energy harvester.

Parameter	Value	Parameter	Value
K_e	0.77N-m/A	F_c	160N
R_c	2.41Ω	m_s	3000kg
l	2.55×10^{-3}m/rad	c_s	395N-s/m
m_d	20kg	k_s	3×10^4N/s
c_d	575N-s/m	ω_a	0.5Hz
k_d	630N/m	σ_a	0.25m/s^2

We assume that the input $w(t)$ is a white noise process with spectral intensity equal to unity. In addition, we have that σ_a is the standard deviation of the disturbance acceleration, $\omega_a = \sqrt{k/m}$ is the passband of disturbance filter, and ζ_a determines the quality factor of the disturbance filter. We combine the harvester states with the disturbance states such that the augmented state space $\mathbf{x}(t) = \begin{bmatrix}\mathbf{x}_h^T(t) & \mathbf{x}_a^T(t)\end{bmatrix}^T$ obeys

$$\dot{\mathbf{x}}(t) = \mathbf{A}\mathbf{x}(t) + \mathbf{F}\text{sgn}\left(\dot{x}(t)\right) + \mathbf{B}i(t) + \mathbf{G}w(t) \tag{7a}$$

$$v(t) = \mathbf{B}^T\mathbf{x}(t) \tag{7b}$$

$$\dot{x}(t) = \mathbf{C}\mathbf{x}(t) \tag{7c}$$

with appropriate definitions for the matrices $\{\mathbf{A}, \mathbf{B}, \mathbf{C}, \mathbf{F}, \mathbf{G}\}$ above.

Values for the various parameters considered in this study can be found in Table 1. The transducer parameters values are specific to the EC3 ballscrew and AKM44E motor configuration from Kollmorgen, which were experimentally verified in Cassidy *et al.*[11] In addition, the energy harvester's mass, damping, and stiffness correspond to values for a scaled tuned mass damper within a multi-story building. The system's natural frequency is 0.5Hz, with a damping ratio of 5%.

3. OPTIMAL LINEAR ENERGY HARVESTING

In this section we neglect the effects of the Coulomb friction force in equation (7) (i.e., we assume that $F_c = 0$). In addition, we assume that the power losses in the electronics are quadratic and purely resistive. For the linear harvester and disturbance model, it is then possible to determine the state feedback control law that maximizes the harvested power using LQG optimal control theory. Optimization of an energy harvesting cost function can be accomplished through the linear state feedback relationship $i(t) = \mathbf{K}\mathbf{x}(t)$, with $\mathbf{K}$ derived as explained below.

Operating the transducer such that it implements a desired control law requires power electronic circuitry to accurately track a current command signal. Because the electronics must be capable of injecting as well as extracting power, an H-bridge, pictured in figure 2(a), is used to track the current command signal $i^*(t)$. As shown in figure 2(a), tracking $i^*(t)$ is accomplished through high-frequency pulsewidth modulation (PWM) switching control of four MOSFETs (labeled Q_1 through Q_4). Gate drives control the MOSFETs using an error signal, which is computed by sending the difference between the desired and actual current through a proportional-integral (PI) controller. We make the assumption that the tracking dynamics of the power electronics lie outside the frequency band of the disturbance.

To determine the energy harvesting cost function, we first define the power delivered to storage as the power extracted by the transducer minus the transmission losses in the power electronic circuitry. If we approximate these losses as resistive, with some resistance R, then the power delivered to storage is

$$P_S(t) = -i(t)v(t) - Ri^2(t)\ . \tag{8}$$

We note that the negative signs in this expression are due to the fact that the current flowing into the transducer is defined as being positive in figure 2(a). Next, we define the average power generated as the expectation of the power delivered to storage; i.e.,

$$\bar{P}_{gen} = -\mathcal{E}\left\{ \begin{bmatrix}\mathbf{x}(t)\\ i(t)\end{bmatrix}^T \begin{bmatrix}\mathbf{0} & \frac{1}{2}\mathbf{B}\\ \frac{1}{2}\mathbf{B}^T & R\end{bmatrix} \begin{bmatrix}\mathbf{x}(t)\\ i(t)\end{bmatrix} \right\}. \tag{9}$$

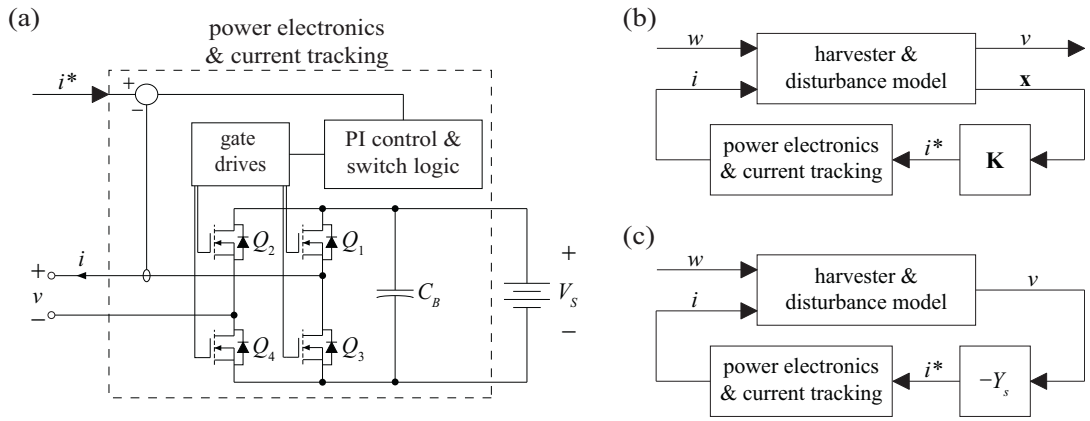

Figure 2. (a) Example power electronic circuit consisting of an H-bridge; (b) block diagram illustrating the state feedback control law; (c) block diagram illustrating the static admittance.

Maximization of equation (9) is equivalent to a LQG optimal control problem.

In order to maximize the expression in equation (9), we must determine the optimal feedback gain matrix $\mathbf{K}$. It has been shown by Scruggs[9] that $\mathbf{K}$ is

$$\mathbf{K} = -\frac{1}{R}\mathbf{B}^T\left(\mathbf{P} + \tfrac{1}{2}\mathbf{I}\right) \tag{10}$$

where $\mathbf{P} = \mathbf{P}^T < 0$ is the unique, stabilizing solution to the nonstandard Riccati equation

$$\mathbf{A}^T\mathbf{P} + \mathbf{P}\mathbf{A} - \frac{1}{R}\left(\mathbf{P} + \tfrac{1}{2}\mathbf{I}\right)\mathbf{B}\mathbf{B}^T\left(\mathbf{P} + \tfrac{1}{2}\mathbf{I}\right) = \mathbf{0}\,. \tag{11}$$

Furthermore, the average power generated with the electronics implementing the optimal feedback control law is

$$\bar{P}_{gen} = -\mathbf{G}^T\mathbf{P}\mathbf{G}\,. \tag{12}$$

A block diagram illustrating the implementation of the optimal state feedback control law can be seen in figure 2(b). In this figure we make the assumption that $i(t) \approx i^*(t)$. In addition, we assume that every state in the augmented harvester and disturbance model is available for feedback. However, if this is not the case, then the measured transducer voltage can be passed through a standard Luenberger observer,[19] which can be used to estimate the remaining system states. It would thus be straightforward to extend the theory presented in this paper to design a dynamic controller that maps the transducer voltage into the current command signal to be tracked by the electronics.

It is also possible to operate the H-bridge such that it imposes a static admittance at the terminals of the transducer. By convention, when the electronics are implementing the static admittance the control current relationship is $i(t) = -Y_s v(t)$. A block diagram illustrating the implementation of the static admittance can be seen in figure 2(c). Again, we make the assumption that $i(t) \approx i^*(t)$. Substituting $i(t) = -Y_s v(t)$ into equation (7) results in the closed-loop dynamics having the form

$$\dot{\mathbf{x}}(t) = \left[\mathbf{A} - Y_s\mathbf{B}\mathbf{B}^T\right]\mathbf{x}(t) + \mathbf{G}w(t)\,. \tag{13}$$

The stationary covariance matrix $\mathbf{S} = \mathcal{E}\{\mathbf{x}(t)\mathbf{x}^T(t)\}$ is found by solving the Lyapunov equation

$$\left[\mathbf{A} - Y_s\mathbf{B}\mathbf{B}^T\right]\mathbf{S} + \mathbf{S}\left[\mathbf{A} - Y_s\mathbf{B}\mathbf{B}^T\right]^T + \mathbf{G}\mathbf{G}^T = \mathbf{0} \tag{14}$$

and the resultant average power generated can be computed as

$$\bar{P}_{gen} = \left(Y_s - Y_s^2 R\right)\mathbf{B}^T\mathbf{S}\mathbf{B}\,. \tag{15}$$

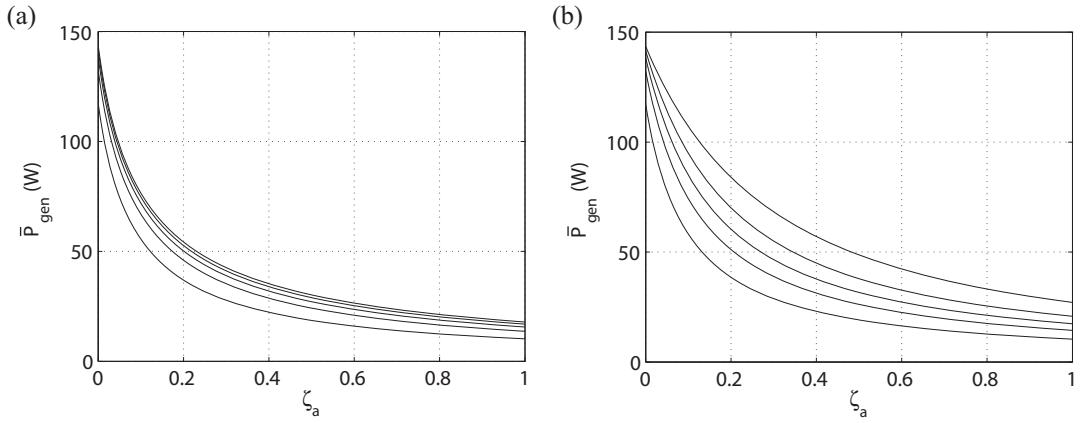

Figure 3. Comparison of the average power generated by: (a) the optimal static admittance and; (b) the optimal feedback control law; for R values of 2Ω, 5Ω, 10Ω, 20Ω, and 50Ω (from top to bottom).

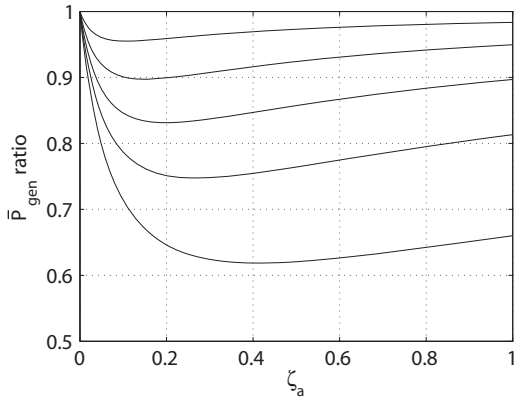

Figure 4. $\bar{P}_{gen}$ ratio for R values of 2Ω, 5Ω, 10Ω, 20Ω, and 50Ω (from bottom to top).

Because the system only has one design parameter (i.e., Y_s) in this case, the most straight-forward way to optimize $\bar{P}_{gen}$ is via a one-dimensional line search. For example, the bisection algorithm will converge rapidly to the optimal Y_s, given $\{\mathbf{A}, \mathbf{B}, \mathbf{G}, R\}$.

We can gain some valuable insight into the linear energy harvesting problem by comparing the $\bar{P}_{gen}$ resulting from the optimal static admittance with the $\bar{P}_{gen}$ resulting from the optimal feedback control law. The plots in figure 3 illustrate this comparison for the SDOF energy harvester characterized by equation (7) with $\mathbf{F} = \mathbf{0}$. We see that the curves in both plots monotonically decrease as ζ_a increases and that the curves in figure 3(b) have higher $\bar{P}_{gen}$ values than the curves in figure 3(a).

To illustrate the improvement in energy harvesting performance, we plot ratio of $\bar{P}_{gen}$ resulting from the optimal static admittance over the $\bar{P}_{gen}$ resulting from the optimal feedback control law in figure 4. From this plot, we obtain the interesting result that there is a finite bandwidth for $a(t)$ at which the full-state feedback control law is most beneficial. Additionally, we see that in the narrowband limit (i.e., as $\zeta_a \to 0$) that both the static admittance and full state feedback harvest the same amount of average power. As pointed out in,[20] this is due to the fact that for the system under consideration, the velocity and acceleration gains are the only gains in $\mathbf{K}$ required for the optimal feedback control law. In the narrowband limit, $\dot{x}(t)$ and $a(t)$ become purely sinusoidal and exactly in phase, which means that knowledge of both is redundant. Thus, we can conclude that for this simplified case, that the optimal $i(t)$ is attained by imposing a static admittance.

4. STATISTICALLY LINEARIZED ENERGY HARVESTING

In this section, we extend the theory presented in the previous section to account for the Coulomb friction force present in the electromagnetic transducer. Again we assume that the losses in the electronics are purely resistive.

4.1 Stationary covariance

The general state space model for an energy harvesting system with nonlinearities introduced by the transducer is

$$\dot{\mathbf{x}}(t) = \mathbf{A}\mathbf{x}(t) + \phi(\mathbf{x}(t), t) + \mathbf{B}i(t) + \mathbf{G}w(t) \tag{16a}$$

$$v(t) = \mathbf{B}^T\mathbf{x}(t) \tag{16b}$$

$$y(t) = \mathbf{C}\mathbf{x}(t) \tag{16c}$$

where we assume the function $\phi(\mathbf{x}(t), t)$ is nonlinear. We assume $\phi(\mathbf{0}, t) = \mathbf{0}$, and that it is anti-symmetric; i.e., $\phi(-\mathbf{x}(t), t) = -\phi(\mathbf{x}(t), t)$. In addition, we assume that $\mathbf{x}(t)$ has a stationary probability distribution which can be approximated as Gaussian with zero mean (because $\phi(\mathbf{x}(t), t)$ is assumed to be anti-symmetric) and covariance $\mathbf{S}$. The corresponding stationary probability density function (pdf) is

$$p(\mathbf{x}(t), t) = \frac{1}{\sqrt{(2\pi)^n \ \det\mathbf{S}}} \ \exp\{-\tfrac{1}{2}\mathbf{x}^T(t)\mathbf{S}^{-1}\mathbf{x}(t)\} \ . \tag{17}$$

If we implement any stabilizing full-state feedback control law $i(t) = \mathbf{K}\mathbf{x}(t)$, then the solution to the stationary covariance $\mathbf{S}$ can be found via statistical linearization.[21] The equation that $\mathbf{S}$ must satisfy in stationarity is

$$\mathcal{E}\{\nabla_{\mathbf{x}}^T\phi_{cl}^T(\mathbf{x}(t), t)\}^T\mathbf{S} + \mathbf{S} \ \mathcal{E}\{\nabla_{\mathbf{x}}^T\phi_{cl}^T(\mathbf{x}(t), t)\} + \mathbf{G}\mathbf{G}^T = \mathbf{0} \tag{18}$$

where the closed-loop nonlinear function $\phi_{cl}(\mathbf{x}(t), t)$ is

$$\phi_{cl}(\mathbf{x}(t), t) = \mathbf{A}\mathbf{x}(t) + \mathbf{B}\mathbf{K}\mathbf{x}(t) + \phi(\mathbf{x}(t), t) \tag{19}$$

and where $\nabla_{\mathbf{x}}$ is the gradient operator with respect to the variable $\mathbf{x}$.

For the case where the nonlinearity is Coulomb friction, we replace $\phi(\mathbf{x}(t), t)$ with $\mathbf{F}\text{sgn}\{\dot{x}(t)\}$ in equation (19) where $\dot{x}(t) = y(t)$. Taking the gradient of $\phi_{cl}(\mathbf{x}(t), t)$ with respect to $\mathbf{x}(t)$, results in

$$\nabla_{\mathbf{x}}^T\phi_{cl}^T(\mathbf{x}(t), t) = \mathbf{A}^T + \mathbf{K}^T\mathbf{B}^T + 2\mathbf{C}^T\mathbf{F}^T\delta\left(y(t)\right) \tag{20}$$

where $\delta(\cdot)$ is the Dirac delta function. Next, taking the expectation of both sides of equation (20) results in the following expression

$$\mathcal{E}\{\nabla_{\mathbf{x}}^T\phi_{cl}^T(\mathbf{x}(t), t)\} = \mathbf{A}^T + \mathbf{K}^T\mathbf{B}^T + 2\mathbf{C}^T\mathbf{F}^T\int_y \delta(y(t))p(y(t), t) \ dy \ . \tag{21}$$

But by assumption, the pdf for $y(t)$ is a zero-mean Gaussian function, with scalar variance $s_y = \mathbf{C}\mathbf{S}\mathbf{C}^T$; i.e.,

$$p(y(t), t) = \frac{1}{\sqrt{2\pi s_y}} \ \exp\{-y^2(t)/2s_y\} \ . \tag{22}$$

Thus, we have that equation (21) is

$$\mathcal{E}\{\nabla_{\mathbf{x}}^T\phi_{cl}^T(\mathbf{x}(t), t)\} = \mathbf{A}^T + \mathbf{K}^T\mathbf{B}^T + \mathbf{V}^T \tag{23}$$

where

$$\mathbf{V} = \sqrt{\frac{2}{\pi}} \ \frac{\mathbf{F}\mathbf{C}}{\sqrt{\mathbf{C}\mathbf{S}\mathbf{C}^T}} \ . \tag{24}$$

Substituting equation (23) into equation (18) results in an equation for $\mathbf{S}$ as

$$\left[\bar{\mathbf{A}} + \mathbf{B}\mathbf{K}\right]\mathbf{S} + \mathbf{S}\left[\bar{\mathbf{A}} + \mathbf{B}\mathbf{K}\right]^T + \mathbf{G}\mathbf{G}^T = \mathbf{0} \tag{25}$$

where $\bar{\mathbf{A}} = \mathbf{A} + \mathbf{V}$. It is important to note that the matrix $\mathbf{V}$ augments the dynamics matrix $\mathbf{A}$ by adding an additional term which supplements the viscous damping in the system. This additional term is the statistically-equivalent linear viscous damping due to the Coulomb friction force. Also, note that although equation (25) is reminiscent of a Lyapunov equation, it is in fact nonlinear, because $\mathbf{V}$ depends on $\mathbf{S}$. In general, the solution to equation (25) can only be found iteratively.

4.2 Stationary optimal energy harvesting

Recall that the energy harvesting objective is to maximize the average power generated; i.e.,

$$\bar{P}_{gen} = -\mathrm{tr}\{\, [\tfrac{1}{2}\mathbf{K}^T\mathbf{B}^T + \tfrac{1}{2}\mathbf{B}\mathbf{K} + R\mathbf{K}^T\mathbf{K}]\, \mathbf{S}\} \tag{26}$$

over the feedback gain matrix $\mathbf{K}$. Since this optimization is subject to the constraint in equation (25), we define the Hamiltonian $\mathcal{H}$ as

$$\mathcal{H} = -\bar{P}_{gen} + \mathrm{tr}\left\{\mathbf{P}\left(\left[\bar{\mathbf{A}} + \mathbf{B}\mathbf{K}\right]\mathbf{S} + \mathbf{S}\left[\bar{\mathbf{A}} + \mathbf{B}\mathbf{K}\right]^T + \mathbf{G}\mathbf{G}^T\right)\right\} \tag{27}$$

where $\mathbf{P} = \mathbf{P}^T$ is a Lagrange multiplier matrix which enforces equation (25) as a constraint in the optimization. Thus, we have the following minimax problem

$$\mathbf{K} = \underset{\mathbf{K}}{\mathrm{argmin}} \left[\min_{\mathbf{S}=\mathbf{S}^T} \max_{\mathbf{P}=\mathbf{P}^T} \mathcal{H}\right] . \tag{28}$$

To find the optimal solution to the problem in equation (28), we take the partial derivative of the Hamiltonian with respect to each of the decision variables and set these quantities equal to zero. This procedure constitutes a standard approach to solving an optimal control problem.[22] For brevity, we suppress the intermediate steps required to compute the partial derivatives and merely highlight their final analytical expressions. We start by taking the partial derivative of $\mathcal{H}$ with respect to $\mathbf{S}$; i.e.,

$$\frac{\partial \mathcal{H}}{\partial \mathbf{S}} = \tfrac{1}{2}\mathbf{K}^T\mathbf{B}^T + \tfrac{1}{2}\mathbf{B}\mathbf{K} + R\mathbf{K}^T\mathbf{K} + \mathbf{P}\left[\bar{\mathbf{A}} + \mathbf{B}\mathbf{K}\right] + \left[\bar{\mathbf{A}} + \mathbf{B}\mathbf{K}\right]^T\mathbf{P} - \mathbf{U}\mathbf{P}\mathbf{V} - \mathbf{V}^T\mathbf{P}\mathbf{U}^T = \mathbf{0} \tag{29}$$

where

$$\mathbf{U} = \frac{1}{2}\,\frac{\mathbf{C}^T\mathbf{C}\mathbf{S}}{\mathbf{C}\mathbf{S}\mathbf{C}^T} . \tag{30}$$

Next, we take the partial derivative of $\mathcal{H}$ with respect to $\mathbf{K}$; i.e.,

$$\frac{\partial \mathcal{H}}{\partial \mathbf{K}} = \mathbf{S}\mathbf{B}^T + 2R\mathbf{S}\mathbf{K}^T + 2\mathbf{S}\mathbf{P}\mathbf{B} = \mathbf{0} . \tag{31}$$

Pre-multiplying equation (31) by $\mathbf{S}^{-1}$ and solving for $\mathbf{K}$ results in equation (10), but with the new $\mathbf{P}$ found via equation (29) rather than the Riccati equation in equation (11). It is not necessary to take the partial derivative of $\mathcal{H}$ with respect to the Lagrange multiplier $\mathbf{P}$ as this will just give us back the constraint in equation (25). Finally, we can substitute equation (10) into equations (25) and (29) to arrive at two coupled, nonlinear algebraic equations for $\mathbf{S}$ and $\mathbf{P}$ that must hold at the optimum; i.e.,

$$\left[\bar{\mathbf{A}} - \frac{1}{R}\mathbf{B}\mathbf{B}^T\left(\mathbf{P} + \tfrac{1}{2}\mathbf{I}\right)\right]\mathbf{S} + \mathbf{S}\left[\bar{\mathbf{A}} - \frac{1}{R}\mathbf{B}\mathbf{B}^T\left(\mathbf{P} + \tfrac{1}{2}\mathbf{I}\right)\right]^T + \mathbf{G}\mathbf{G}^T = \mathbf{0} \tag{32}$$

$$\bar{\mathbf{A}}^T\mathbf{P} + \mathbf{P}\bar{\mathbf{A}} - \frac{1}{R}\left(\mathbf{P} + \tfrac{1}{2}\mathbf{I}\right)\mathbf{B}\mathbf{B}^T\left(\mathbf{P} + \tfrac{1}{2}\mathbf{I}\right) - \mathbf{U}\mathbf{P}\mathbf{V} - \mathbf{V}^T\mathbf{P}\mathbf{U}^T = \mathbf{0} . \tag{33}$$

4.3 Iterative algorithm

Because $\mathbf{U}$ and $\mathbf{V}$ depend on $\mathbf{S}$, equations (32) and (33) are coupled nonlinear algebraic equations. As such, solutions for the stationary covariance matrix $\mathbf{S}$ and the Lagrange multiplier $\mathbf{P}$ must be computed iteratively. To do this, we begin by linearizing equation (27) about $\mathbf{S} = \mathbf{S}_0$; i.e.,

$$\tilde{\mathcal{H}} = -\bar{P}_{gen} + \mathrm{tr}\left\{\mathbf{P}\Big[\,[\mathbf{A} + \mathbf{B}\mathbf{K} + \mathbf{V}_0]\,\mathbf{S} + \mathbf{S}\,[\mathbf{A} + \mathbf{B}\mathbf{K} + \mathbf{V}_0] + \mathbf{G}\mathbf{G}^T + \tfrac{1}{2}\left(\mathbf{V}_0\mathbf{S}_0 + \mathbf{S}_0\mathbf{V}_0^T\right)\left(1 - \tfrac{\mathbf{C}\mathbf{S}\mathbf{C}^T}{\mathbf{C}\mathbf{S}_0\mathbf{C}^T}\right)\Big]\right\} \tag{34}$$

where $\mathbf{V}_0 = \mathbf{V}|_{\mathbf{S}=\mathbf{S}_0}$. Regrouping terms, we have that

$$\begin{aligned}\tilde{\mathcal{H}} = \mathrm{tr}\Big\{\mathbf{P}\left[\mathbf{G}\mathbf{G}^T + \tfrac{1}{2}\left(\mathbf{V}_0\mathbf{S}_0 + \mathbf{S}_0\mathbf{V}_0^T\right)\right] + \mathbf{S}\Big[&\tfrac{1}{2}\mathbf{K}^T\mathbf{B}^T + \tfrac{1}{2}\mathbf{B}\mathbf{K} + R\mathbf{K}^T\mathbf{K} + \mathbf{P}\,[\mathbf{A} + \mathbf{B}\mathbf{K} + \mathbf{V}_0] \\ &+ [\mathbf{A} + \mathbf{B}\mathbf{K} + \mathbf{V}_0]^T\mathbf{P} - \mathbf{U}_0\mathbf{P}\mathbf{V}_0 - \mathbf{V}_0^T\mathbf{P}\mathbf{U}_0^T\Big]\Big\}\end{aligned} \tag{35}$$

where $\mathbf{U}_0 = \mathbf{U}|_{\mathbf{S}=\mathbf{S}_0}$. If $\{\mathbf{K}, \mathbf{P}, \mathbf{S}\}$ are the optimal parameters for original problem, they will also be optimal parameters for the linearized problem with $\mathbf{S}_0$ equal to its optimal value.

Now, consider that if we assume that the optimal $\mathbf{K}$ is such that $\mathbf{A}+\mathbf{BK}+\mathbf{V}$ is asymptotically stable, then $\mathbf{S}_0 > 0$ can be assumed to hold at the optimal solution as well. If this is the case then, using the linearized Hamiltonian and substituting the optimal relationship between $\mathbf{K}$ and $\mathbf{P}$ in equation (10), the value of $\tilde{\mathcal{H}}$ is bounded by

$$\tilde{\mathcal{H}} > \mathrm{tr}\left\{\mathbf{P}\left[\mathbf{G}\mathbf{G}^T + \tfrac{1}{2}\left(\mathbf{V}_0\mathbf{S}_0 + \mathbf{S}_0\mathbf{V}_0^T\right)\right]\right\} \tag{36}$$

where $\mathbf{P}$ is subjected to the constraint

$$\left[\mathbf{A}+\mathbf{V}_0\right]^T\mathbf{P} + \mathbf{P}\left[\mathbf{A}+\mathbf{V}_0\right] - \mathbf{U}_0\mathbf{P}\mathbf{V}_0 - \mathbf{V}_0^T\mathbf{P}\mathbf{U}_0^T - \frac{1}{R}\left(\mathbf{P}+\tfrac{1}{2}\mathbf{I}\right)\mathbf{B}\mathbf{B}^T\left(\mathbf{P}+\tfrac{1}{2}\mathbf{I}\right) > 0\,. \tag{37}$$

Furthermore, we know from equation (33) that for any optimal solution, equation (37) holds with an equality. But if this is true, then equation (36) also holds with an equality at any optimum. Thus, for $\mathbf{S}_0 > 0$ equal to the optimal $\mathbf{S}$, the optimization

$$\mathbf{P} = \underset{\mathbf{P}}{\mathrm{argmax}}\,\mathrm{tr}\left\{\mathbf{P}\left[\mathbf{G}\mathbf{G}^T + \tfrac{1}{2}\left(\mathbf{V}_0\mathbf{S}_0 + \mathbf{S}_0\mathbf{V}_0^T\right)\right]\right\} \tag{38}$$

subject to equation (37), or equivalently, the LMI

$$\begin{bmatrix}\left[\mathbf{A}+\mathbf{V}_0\right]^T\mathbf{P} + \mathbf{P}\left[\mathbf{A}+\mathbf{V}_0\right] - \mathbf{U}_0\mathbf{P}\mathbf{V}_0 - \mathbf{V}_0^T\mathbf{P}\mathbf{U}_0^T & \left(\mathbf{P}+\frac{1}{2}\mathbf{I}\right)\mathbf{B} \\ \mathbf{B}^T\left(\mathbf{P}+\frac{1}{2}\mathbf{I}\right) & R\end{bmatrix} > 0 \tag{39}$$

will give the same optimal solution for $\mathbf{P}$.

Motivated by the above, we define the matrix function $\mathbf{P} = \Theta(\mathbf{S}_0)$, over the domain $\mathbf{S}_0 > 0$, as

$$\Theta(\mathbf{S}_0) = \underset{\mathbf{P}}{\mathrm{sol}}\begin{cases}\text{Given :} & \mathbf{S}_0 > 0 \\ \text{Maximize :} & \mathrm{tr}\left\{\mathbf{P}\left[\mathbf{G}\mathbf{G}^T + \frac{1}{2}\left(\mathbf{V}_0\mathbf{S}_0 + \mathbf{S}_0\mathbf{V}_0^T\right)\right]\right\} \\ \text{Over :} & \mathbf{P} \\ \text{Subject to :} & \text{LMI constraint (39)}\end{cases} \tag{40}$$

The optimization in equation (40) is convex and is feasible for any $\mathbf{S}_0 > 0$, and may therefore be viewed as a unique function over the domain $\mathbf{S}_0 > 0$. Using this function, the following iterative algorithm can be used to solve for the values of $\mathbf{S}$ and $\mathbf{P}$ at the optimum:

Step 0: Initialize $\mathbf{S}_0$ by solving the linear energy harvesting problem (i.e., with $\mathbf{U} = \mathbf{V} = \mathbf{0}$).

Step 1: Compute new values for $\mathbf{V}_0$ and $\mathbf{U}_0$ using $\mathbf{S}_0$.

Step 2: Compute $\mathbf{P} = \Theta(\mathbf{S}_0)$.

Step 3: In equation (32), fix $\mathbf{V} \leftarrow \mathbf{V}_0$ and solve the resultant Lyapunov equation for $\mathbf{S}$.

Step 4: Set $\mathbf{S}_0 \leftarrow \mathbf{S}$ and return to Step 1.

Convergence of the algorithm is reached when the absolute value of the change in $\bar{P}_{gen}$ between the current and previous iteration is below a certain tolerance. The value of $\bar{P}_{gen}$ at the first iteration can be calculated using equation (12) while the value of $\bar{P}_{gen}$ at any subsequent iteration can be calculated using equation (26).

Here, we make no claim that this algorithm always converges, although it did converge for all examples considered in this paper. Once convergence is reached, asymptotic stability of $\mathbf{A}+\mathbf{BK}+\mathbf{V}$ at the optimum should be verified. Furthermore, it should also be verified that the matrix $\mathbf{A}+\mathbf{BK}$ is also asymptotically stable. For the Coulomb friction nonlinearity considered here, this condition guarantees that all state trajectories in the response ensemble are bounded. This second stability condition does not appear to be guaranteed by the

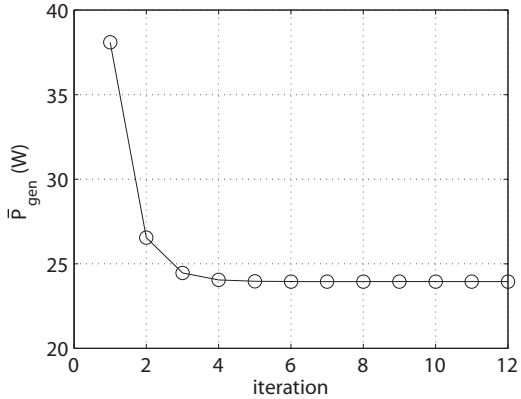

Figure 5. Example of the iterative algorithm converging for $R = 5\Omega$ and $\zeta_a = 0.5$.

first, and both are necessary for the resultant optimal controller to be valid. Both conditions were found to hold uniformly in the examples considered here.

For the energy harvesting example considered in this paper, the above algorithm was found to converge within 10–20 iterations. Using the system defined in equation (7), we illustrate the convergence of the proposed algorithm in figure 5. For this example, we fix $R = 5\Omega$ and $\zeta_a = 0.5$ and run the algorithm with a convergence tolerance of $1e^{-6}$. As shown, the algorithm converges to $\bar{P}_{gen} = 23.9$W in 12 iterations.

4.4 Example

We illustrate the average power generated by the SDOF energy harvester using the optimal static admittance and optimal state feedback control law in figure 6. Including the Coulomb friction results in the performance of both the static admittance and state feedback control law being approximately 40% of the performance of the linear energy harvester. The plot of the $\bar{P}_{gen}$ ratio in figure 7 illustrates the improvement in energy harvesting performance through the use of the state feedback control law. An important result of this analysis can be seen in the narrowband limit as $\zeta_a \to 0$. At this limit, we see that the $\bar{P}_{gen}$ ratio is no longer equal to unity, as it was for the linear energy harvester. In other words, for narrowband but still stochastic disturbances, the optimal controller is no longer just voltage feedback. This is interesting because if $a(t)$ were purely sinusoidal, voltage feedback would indeed be optimal. This tells us that if we include the effects of Coulomb friction, a narrowband disturbance is distinct from a harmonic disturbance, irrespective of its quality factor.

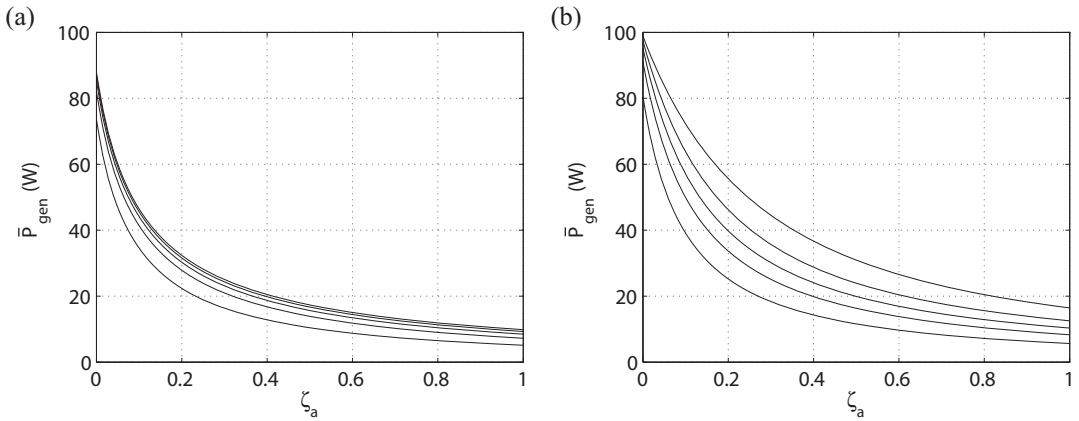

Figure 6. Comparison of the average power generated by: (a) the optimal static admittance and; (b) the optimal feedback control law; for R values of 2Ω, 5Ω, 10Ω, 20Ω, and 50Ω (from top to bottom).

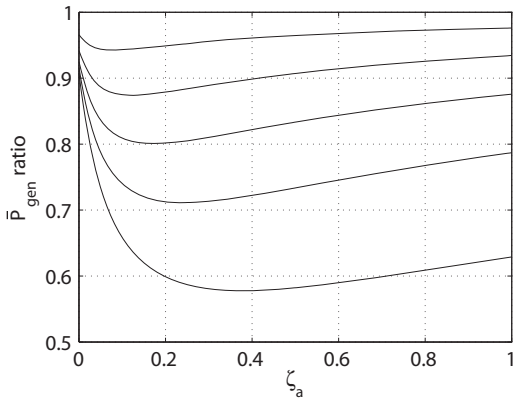

Figure 7. $\bar{P}_{gen}$ ratio for R values of 2Ω, 5Ω, 10Ω, 20Ω, and 50Ω (from bottom to top).

5. CONCLUSIONS

In order to fully maximize the potential power generation from an actively controlled vibratory energy harvester, the nonlinearities in the system must be accounted for in the control design. Nonlinearities arising in the dynamics of the vibratory system can be statistically linearized if the system is excited by a stochastic disturbance and its response is approximated by a Gaussian distribution. This paper illustrates how to account for the Coulomb friction present in a stochastically excited SDOF oscillator and maximize the average power generation by simultaneously solving two coupled nonlinear algebraic equations. These equations are derived from first principles and an iterative algorithm is proposed to solve for the statistically linearized covariance matrix as well as the optimal feedback gain matrix. For the statistically linearized energy harvesting system with purely resistive losses, it is shown that optimal full-state feedback generates more average power than the optimal static admittance for a narrowband disturbance. This result is in contrast to the linear SDOF energy harvesting system, for which these two control techniques are equivalent in the narrowband limit.

ACKNOWLEDGMENTS

This work was supported by NSF award CMMI-0747563. The views expressed in this article are those of the authors, and do not necessarily reflect those of the National Science Foundation.

REFERENCES

[1] Roundy, S., Wright, P. K., and Rabaey, J., "A study of low level vibrations as a power source for wireless sensor nodes," *Journal of Computer Communications* **26**, 1131–1144 (2002).

[2] Zuo, L., Scully, B., Shestani, J., and Zhou, Y., "Design and characterization of an electromagnetic energy harvester for vehicle suspensions," *Smart Materials and Structures* **19** (2010). #045003.

[3] Nagode, C., Ahmadian, M., and Taheri, S., "Effective energy harvesting devices for railroad applications," *Proc. SPIE 7643* (2010).

[4] Scruggs, J. T. and Jacob, P., "Harvesting ocean wave energy," *Science* **323**, 1176–1178 (2009).

[5] Ni, T., Zuo, L., and Kareem, A., "Assessment of energy potential and vibration mitigation of regenerative tuned mass dampers on wind excited tall buildings," *Proc. ASME IDETC* (2011).

[6] Lefeuvre, E., Audigier, D., Richard, C., and Guyomar, D., "Buck-boost converter for sensorless power optimization of piezoelectric energy harvester," *IEEE Transactions on Power Electronics* **22**, 2018–2025 (2007).

[7] Liu, Y., Tian, G., Wang, Y., Lin, J., Zhang, Q., and Hofmann, H. F., "Active piezoelectric energy harvesting: general principle and experimental demonstration," *Journal of Intelligent Material Systems and Structures* **20**, 575–585 (2009).

[8] Stephen, N. G., "On energy harvesting from ambient vibration," *Journal of Sound and Vibration* **293**, 409–425 (2006).

[9] Scruggs, J. T., "On the causal power generation limit for a vibratory energy harvester in broadband stochastic response," *Journal of Intelligent Material Systems and Structures* **21**, 1249–1262 (2010).

[10] Stanton, S. C., Erturk, A., Mann, B. P., and Inman, D. J., "Nonlinear piezoelectricity in electroelastic energy harvesters: Modeling and experimental identification," *Journal of Applied Physics* **108** (2010). #074903.

[11] Cassidy, I. L., Scruggs, J. T., Behrens, S., and Gavin, H. P., "Design and experimental characterization of an electromagnetic transducer for large-scale vibratory energy harvesting applications," *Journal of Intelligent Material Systems and Structures* **22**, 2009–2024 (2011).

[12] Ali, S. F., Adhikari, S., Friswell, M. I., and Narayanan, S., "The analysis of piezomagnetoelastic energy harvesters under broadband random excitations," *Journal of Applied Physics* **109** (2011). #074904.

[13] Wonham, W. M. and Cashman, W. F., "A computational approach to optimal control of stochastic saturating systems," *International Journal of Control* **10**, 77–98 (1969).

[14] Gökçek, C., Kabamba, P. T., and Meerkov, S. M., "An lqr/lqg theory for systems with saturating actuators," *IEEE Transactions on Automatic Control* **46**, 1529–1542 (2001).

[15] Narayanan, S. and Senthil, S., "Stochastic optimal active control of a 2-dof quarter car model with non-linear passive suspension elements," *Journal of Sound and Vibration* **211**, 495–506 (1998).

[16] Ying, Z. G., Ni, Y. Q., and Ko, J. M., "Semi-active optimal control of linearized systems with multi-degree of freedom and application," *Journal of Sound and Vibration* **279**, 373–388 (2005).

[17] Boyd, S., El Ghaoui, L., Feron, E., and Balakrishnan, V., [*Linear Matrix Inequalities in System and Control Theory*], SIAM, Philadelphia, PA (1994).

[18] Kollmorgen, "Kollmorgen linear positioners catalog," (2010). Available at: http://www.kollmorgen.com.

[19] Luenberger, D. G., "An introduction to observers," *IEEE Transactions on Automatic Control* **16**, 596–602 (1971).

[20] Cassidy, I. L., Scruggs, J. T., and Behrens, S., "Optimization of partial-state feedback for vibratory energy harvesters subjected to broadband stochastic disturbances," *Smart Materials and Structures* **20** (2011). #085019.

[21] Roberts, J. B. and Spanos, P. D., [*Random Vibration and Statistical Linearization*], Dover, Mineola, NY (2003).

[22] Lewis, F. L. and Syrmos, V. L., [*Optimal Control*], Wiley-Interscience, New York, NY (1995).